Decision Feedback Equalizer for DS-UWB Systems

Oh-Soon Shin* ***Regular Member***

ABSTRACT

Direct-sequence ultra-wideband (DS-UWB) system is being considered as one of promising transmission technologies for wireless personal area networks (WPANs). Due to relatively low spreading factors and huge bandwidth of transmit signal, a DS-UWB receiver needs to be equipped not only with a rake receiver but also with an equalizer, of which the equalizer is not required for traditional direct-sequence code division multiple access (DS-CDMA) systems. The number of rake fingers is limited in practice, influencing the performance of the subsequent equalizer. In this paper, we derive a decision feedback equalizer (DFE) for DS-UWB systems based on the minimum mean square error (MMSE) criterion, and investigate the impact of various parameters on the DFE performance in realistic scenarios. In particular, we propose an approach to improving the performance of the DFE using additional channel estimates for multipaths not combined in the rake receiver, and discuss how the accuracy of channel estimation affects desirable DFE configuration. Moreover, we present simulation results that show the impact of turbo equalization on the DFE performance.

Key Words : Decision Feedback Equalizer (DFE), Direct-sequence Ultra-wideband (DS-UWB), Minimum Mean Square Error (MMSE), Rake Receiver, Wireless Personal Area Network (WPAN)

Ⅰ. Introduction

Ultra-wideband (UWB) radio communications have attracted growing attention due to its promising capability to provide high data rate with low cost and low power consumption [1],[2]. In February 2002, the Federal Communications Commission (FCC) allocated a spectrum from 3.1 GHz to 10.6 GHz for unlicensed use of UWB devices[3]. The FCC also defined UWB signals as having -10 dB bandwidth greater than 500 MHz. This landmark ruling has greatly increased interest in commercial applications of UWB radio, and opened up new opportunities to develop UWB technologies alternative to the classical impulse radio approach in[4]. As a result, UWB is emerging as a viable solution for a short-range indoor wireless network. The IEEE 802.15 Task Group 3a had developed a physical layer standard based on UWB technologies to support high data rate for wireless personal area networks (WPANs)[5]. The standardization has produced two alternative technologies that are supported by various industry groups: direct-sequence UWB (DS-UWB)[6], and multi-band orthogonal frequency division multiplexing (MB-OFDM)[7].

The DS-UWB system is based on direct-sequence spread-spectrum (DS-SS) technology[6]. Each data symbol is spread by a specific spreading code to form a transmit chip sequence. A rake receiver can collect signal energy scattered over multiple chips and multipaths, achieving a processing gain and a form of diversity. Furthermore, DS-SS is inherently capable of mitigating mutual interference between simultaneously operating piconets. One notable disadvantage of the DS-UWB system is that the inter-symbol interference (ISI) can severely degrade the performance, since the transmission bandwidth is huge and the spreading factor is relatively small for high data rates as compared with that of traditional

※ 본 연구는 숭실대학교 교내연구비 지원으로 이루어졌음.
* 숭실대학교 정보통신전자공학부(osshin@ssu.ac.kr)
논문번호 : KICS2008-01-043, 접수일자 : 2008년 1월 21일, 최종논문접수일자 : 2008년 5월 12일

DS-SS systems[8]. This necessitates an equalizer at the DS-UWB receiver.

The focus of this paper is on equalization for DS-UWB systems. In [9], various equalization schemes were investigated. Linear equalization was found to yield unsatisfactory performance, especially when the data rate is high and/or frequency selectivity of the channel is high. Consequently, nonlinear equalization is desired to support high data rates in highly frequency-selective channels. Decision feedback equalizer (DFE) is a practical nonlinear equalizer that compromises between the performance and complexity of the receiver. In this paper, we first derive a DFE based on the minimum mean square error (MMSE) criterion in the context of DS-UWB. Then, we look into the impact of various parameters, such as the number of rake fingers and the number of filter taps, on the DFE performance. In particular, we propose a strategy of exploiting additional channel estimates to improve the DFE performance, and investigate the performance improvement of the MMSE-DFE owing to the use of a turbo equalization structure[10].

This paper is organized as follows. In Section II, we briefly describe the DS-UWB system including the transmitter and receiver structures. In Section III, we derive an explicit form of MMSE-DFE, and propose a strategy for improving the equalization performance with limited rake fingers. Simulation results are presented in Section IV, and conclusions are drawn in Section V.

II. DS-UWB System

As illustrated in Fig. 1, the DS-UWB system divides the available spectrum into two separate bands[6]: a lower band (3.1-4.85 GHz) and a higher band (6.2-9.7 GHz). The use of U-NII bands (5.15-5.35 GHz and 5.725-5.825 GHz) is intentionally avoided to prevent interference between UWB and the existing IEEE 802.11a devices. Channels are distinguished via different offsets in the chip rate and center frequency as well as different spreading codes. Six channels are defined for each band. A physical layer (PHY) frame is

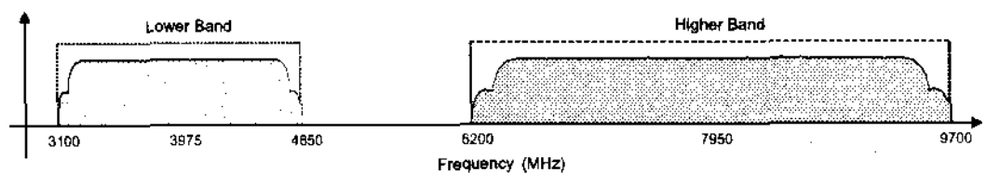

Fig. 1. Frequency plan of the DS-UWB system.

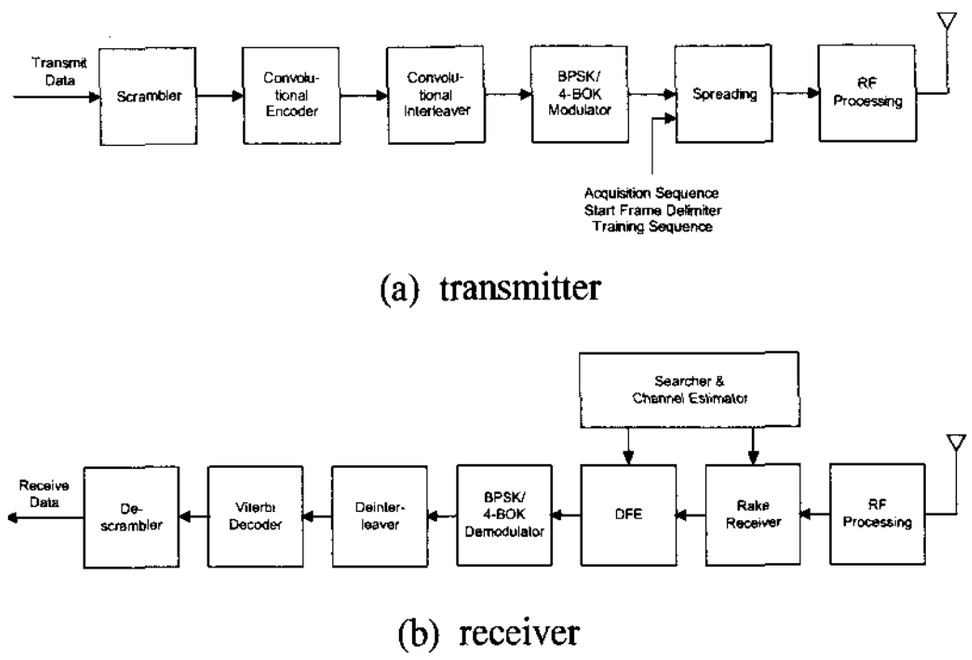

(a) transmitter

(b) receiver

Fig. 2. Block diagram of the DS-UWB transceiver.

composed of a preamble, PHY header, MAC header, header check sequence, data payload, frame check sequence, and tail and pad bits. The preamble is divided into the acquisition sequence, start frame delimiter, and training sequence, and the length of the preamble is allowed to vary according to channel conditions.

Fig. 2(a) illustrates the overall structure of the DS-UWB transmitter. A block of transmit data is scrambled, encoded, interleaved, and modulated prior to spreading. Two types of convolutional encoders are defined: one is associated with a generator polynomial (65_8, 57_8) and constraint length 6, and the other with a generator polynomial (15_8, 17_8) and constraint length 4. The encoders support code rate 1/2 and 3/4. The code rate 3/4 is derived from a baseline rate 1/2 encoder with an appropriate puncturing. The encoded data are interleaved by a convolutional interleaver, and modulated using binary phase shift keying (BPSK) or 4-ary bi-orthogonal keying (4-BOK). Each modulated data symbol is spread by a specific spreading code to form a transmit chip sequence. The length of the spreading code (i.e., the spreading factor, SF) is between 1 and 24. The combinations of the SF, code rate, and modulation scheme determine a set of eight supportable data rates, as given in Table 1 for the lower band.

Table 1. Supportable data rates of the DS-UWB system for the lower band.

Data Rate	BPSK Modulation		4-BOK Modulation	
	Code Rate	SF	Code Rate	SF
28 Mbps	1/2	24	N/A	N/A
55 Mbps	1/2	12	N/A	N/A
110 Mbps	1/2	6	1/2	12
220 Mbps	1/2	3	1/2	6
500 Mbps	3/4	2	3/4	4
660 Mbps	1	2	1	4
1000 Mbps	3/4	1	3/4	2
1320 Mbps	1	1	1	2

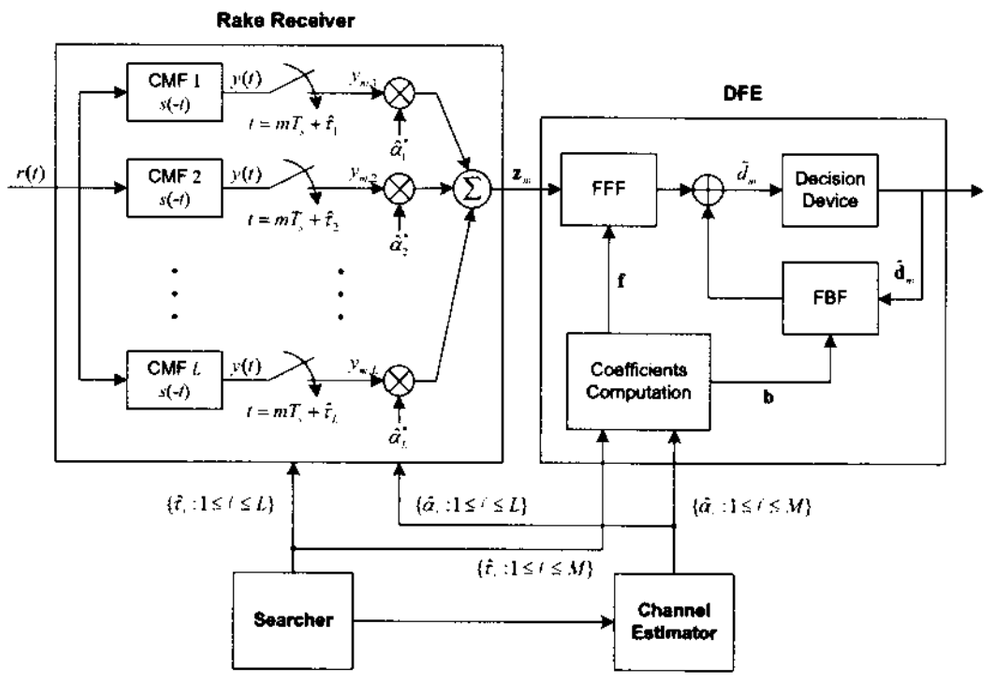

Fig. 3. Rake receiver and DFE structures for the DS-UWB system.

The receiver structure assumed for the DS-UWB system is illustrated in Fig. 2(b). After timing acquisition and channel estimation are done, the chip matched filter (CMF) and the rake receiver despread the received chip sequences arriving from several multipaths, and combine them using maximal ratio combining (MRC). The rake receiver is assumed to collect signal energy from the L strongest received paths. The number of rake fingers will be determined considering the portion of collectable signal energy and complexity of the receiver. A DFE is employed to suppress the ISI in the output of the rake receiver, as suggested in [8]. The detailed structure of the rake receiver and DFE is depicted in Fig. 3. The tap coefficients of the DFE are computed according to the MMSE criterion. After equalization, the signal is demodulated, deinterleaved, soft-decision Viterbi decoded, and descrambled to recover the transmit data.

Ⅲ. MMSE-DFE for DS-UWB Systems

In Section III-1, we describe DS-UWB signals to derive the output of the rake receiver, which goes into the DFE. In Section III-2, we derive an explicit form of MMSE-DFE, and in Section III-3, we identify a determining parameter of the MMSE-DFE, and discuss how to improve the performance of the MMSE-DFE using the parameter.

3.1 Signal Description

The lowpass equivalent of DS-UWB transmit signal can be expressed as

$$x(t)=\sqrt{P}\sum_{n=-\infty}^{\infty}d_n s(t-nT_s), \tag{1}$$

where P is the transmit power, $\{d_n\}$ is BPSK-modulated transmit data sequence, $s(t)=\sum_{i=0}^{SF-1}c_i p(t-iT_c)$ is a spreading waveform, SF is the spreading factor, $\{c_i\}$ is a spreading sequence, T_s is the symbol duration, $T_c=T_s/SF$ is the chip duration, and $p(t)$ is a square-root raised cosine pulse with roll-off factor β and duration T_c. The transmit signal $x(t)$ will experience a multipath fading channel $h(t)$, which is given as

$$h(t)=\sum_{k=0}^{K-1}\alpha_k\delta(t-\tau_k), \tag{2}$$

where K denotes the number of multipaths, and α_k and τ_k, respectively, represent the complex envelope of the channel response and relative delay for the k -th path. From (1) and (2), the received signal can be written as

$$\begin{aligned} h(t)&=x(t)*h(t)+w(t) \\ &=\sqrt{P}\sum_{n=-\infty}^{\infty}d_n\sum_{k=0}^{K-1}\alpha_k s(t-nT_s-\tau_k)+w(t), \end{aligned} \tag{3}$$

where * denotes the convolution operation, and $w(t)$ represents the additive white Gaussian noise (AWGN) with the variance of σ^2. The received signal in (3) passes through a rake receiver composed of L fingers. Consequently, the output of a CMF at each rake finger is given as

$$y(t)=r(t)*s(-t) \tag{4}$$
$$=\sqrt{P}\sum_{n=-\infty}^{\infty}d_n\sum_{k=0}^{K-1}\alpha_k\int_{-\infty}^{\infty}s(t+v-nT_s-\tau_k)s(v)dv$$
$$+\int_{-\infty}^{\infty}w(t+v)s(v)dv.$$

Let $\hat{\alpha}_\ell$ and $\hat{\tau}_\ell$ denote estimates of channel response and relative delay, respectively, for the ℓ-th strongest path. Note that these estimates can be obtained from channel estimator and searcher blocks in the receiver. As depicted in Fig. 3, in order to detect the m-th transmit symbol d_m, the ℓ-th rake finger takes a sample of the CMF output in (4) at time $t=mT_s+\hat{\tau}_\ell$ as

$$y_{m,\ell}=y(mT_s+\hat{\tau}_\ell)/\sqrt{P} \tag{5}$$
$$=\sum_{n=-\infty}^{\infty}d_n\sum_{k=0}^{K-1}\alpha_k\int_{-\infty}^{\infty}s(v+\hat{\tau}_\ell-\tau_k+(m-n)T_s)$$
$$s(v)dv+w_{m,\ell},$$

where we divide the signal by $\sqrt{P}$ for simplicity of manipulation, and $w_{m,\ell}$ is defined as

$$w_{m,\ell}=\frac{1}{\sqrt{P}}\int_{-\infty}^{\infty}w(mT_s+\hat{\tau}_\ell+v)s(v)dv. \tag{6}$$

The rake receiver eventually combines L samples derived from the L fingers using the MRC. The output of the rake receiver can be expressed as

$$z_m=\sum_{\ell=0}^{L-1}\hat{\alpha}_\ell^*y_{m,\ell}$$
$$=\sum_{n=-\infty}^{\infty}d_n\sum_{\ell=0}^{L-1}\sum_{k=0}^{K-1}\hat{\alpha}_\ell^*\alpha_k\int_{-\infty}^{\infty}s(v+\hat{\tau}_\ell-\tau_k+(m-n)T_s)$$
$$s(v)dv+\sum_{\ell=0}^{L-1}\hat{\alpha}_\ell^*w_{m,\ell}$$
$$=\sum_{n=-\infty}^{\infty}d_n\sum_{\ell=0}^{L-1}\sum_{k=0}^{K-1}\hat{\alpha}_\ell^*\alpha_k\rho_s(\hat{\tau}_\ell-\tau_k+(m-n)T_s)+w_m$$
$$=\sum_{\zeta=-\infty}^{\infty}\gamma_\zeta d_{m-\zeta}+w_m, \tag{7}$$

where

$$\rho_s(\tau)\equiv\int_{-\infty}^{\infty}s(v+\tau)s(v)dv, \tag{8a}$$

$$\gamma_\zeta\equiv\sum_{\ell=0}^{L-1}\sum_{k=0}^{K-1}\hat{\alpha}_\ell^*\alpha_k\rho_s(\hat{\tau}_\ell-\tau_k+\zeta T_s), \tag{8b}$$

$$w_m\equiv\sum_{\ell=0}^{L-1}\hat{\alpha}_\ell^*w_{m,\ell}. \tag{8c}$$

It must be noted that the ISI may not be symmetric, i.e., $\gamma_\zeta\neq\gamma_{-\zeta}$, if $L<K$, due to $K-L$ residual multipath components that are not collected at the rake receiver with L fingers.

3.2 MMSE-DFE

The DFE consists of two finite-tap filters, a feedforward filter (FFF) and a feedback filter (FBF). The input to the FFF is the output sequence of the rake receiver, whereas the input to the FBF is the sequence of decisions on previously detected symbols. Specifically, the output of the DFE for the m-th symbol is given as [11]

$$\widetilde{d_m}=\sum_{j=-F}^{0}f_j^*z_{m-j}+\sum_{j=1}^{B}b_j^*\widehat{d_{m-j}}, \tag{9}$$

where $\{f_{-F},f_{-F+1},\cdots,f_0\}$ denotes filter coefficients of an $(F+1)$-tap FFF, and $\{b_1,b_2,\cdots,b_B\}$ denotes filter coefficients of a B-tap FBF. We can express filter inputs and filter coefficients in vector form as

$$u_m\equiv\begin{bmatrix}z_m\\ \widehat{d_m}\end{bmatrix},\quad g\equiv\begin{bmatrix}f\\ b\end{bmatrix}, \tag{10}$$

where

$$z_m\equiv[z_{m+F}\cdots z_{m+1}\ z_m]^T,$$
$$\widehat{d_m}\equiv[\widehat{d_{m-1}}\ \widehat{d_{m-2}}\cdots\widehat{d_{m-B}}]^T,$$
$$f\equiv[f_{-F}\ f_{-F+1}\cdots f_0]^T,$$
$$b\equiv[b_1\ b_2\cdots b_B]^T.$$

Then, (9) can be rewritten as

$$\widetilde{d_m}=g^Hu_m, \tag{11}$$

where $(\cdot)^H$ denotes the conjugate transpose.

According to the MMSE criterion, we can determine coefficient vector g as [11]

$$g=\arg\min_v E\left[|d_m-v^Hu_m|^2\right] \tag{12}$$
$$=(E[u_mu_m^H])^{-1}E[d_m^*u_m],$$

where $E[\cdot]$ denotes the statistical expectation. Under the assumption that all the previously detected symbols are correct, i.e., $\widehat{d_m}=d_m$, (12) can be written as

$$g=\begin{bmatrix} f \\ b \end{bmatrix}=\begin{bmatrix} E\left[z_m z_m^H\right] & E\left[z_m d_m^H\right] \\ \left(E\left[z_m d_m^H\right]\right)^H & I_B \end{bmatrix}\begin{bmatrix} E\left[d_m^* z_m\right] \\ 0_{B\times 1} \end{bmatrix}, \quad (13)$$

which leads to

$$f=\left(A-BB^H\right)^{-1}c \text{ and } b=-B^H f, \quad (14)$$

where $A\equiv E\left[z_m z_m^H\right]$, $B\equiv E\left[z_m d_m^H\right]$ and $c\equiv E\left[d_m^* z_m\right]$. Each entry of A, B and c can be computed as

$$[A]_{ij}=E\left[z_{m+F-i+1} z_{m+F-j+1}^*\right] \quad (15a)$$
$$=\sum_n \gamma_n \gamma_{n+i-j}^* + \sigma^2\delta(i-j),\ 1\le i,j\le F+1,$$

$$[B]_{ij}=E\left[z_{m+F-i+1} d_{m-j}^*\right]=\gamma_{F+1-(i-j)}, \quad (15b)$$
$$1\le i\le F+1, 1\le j\le B,$$

$$[c]_i=E\left[d_m^* z_{m+F-i+1}\right]=\gamma_{F+1-i}, \quad (15c)$$
$$1\le i\le F+1.$$

3.3 Determining Parameter of MMSE-DFE

From (15a)-(15c), we notice that γ_ζ defined in (8b) determines the coefficients of the MMSE-DFE. To accurately compute γ_ζ, the receiver needs to know both the actual channel parameters, $\{(\alpha_k,\tau_k): 1\le k\le L\}$ and estimates of the channel parameters, $\{(\hat{\alpha}_k,\hat{\tau}_k): 1\le k\le L\}$. However, the receiver practically knows only $\{(\hat{\alpha}_k,\hat{\tau}_k): 1\le k\le L\}$, which are obtained from the channel estimator and searcher blocks, as shown in Fig. 3. Therefore, (8b) should be modified to

$$\gamma_\zeta=\sum_{\ell=0}^{L-1}\sum_{k=0}^{L-1}\hat{\alpha}_\ell^*\hat{\alpha}_k\rho_s(\hat{\tau}_\ell-\hat{\tau}_k+\zeta T_s). \quad (16)$$

Although the rake receiver uses estimates of channel parameters only for the L strongest paths as illustrated in Fig. 3, the estimates for weaker paths may be available at the receiver. This is simply because the channel estimator and searcher blocks need to estimate them to identify the L strongest paths. These additional estimates can be exploited for improving the MMSE-DFE performance without increasing the complexity of the receiver. Assuming that the estimates of channel parameters are available for $M(L\le M\le K)$ strongest paths, we propose to compute γ_ζ as

$$\gamma_\zeta=\sum_{\ell=0}^{L-1}\sum_{k=0}^{M-1}\hat{\alpha}_\ell^*\hat{\alpha}_k\rho_S(\hat{\tau}_\ell-\hat{\tau}_k+\zeta T_s). \quad (17)$$

Note that (17) reduces to (16) in a special case of $M=L$. The performance of the MMSE-DFE is expected to improve as M increases.

Ⅳ. Performance Evaluation

4.1 UWB Channel Models

We will use UWB channel models developed in the IEEE 802.15 channel modeling subcommittee [12]. According to the channel model, the path loss and shadow fading is assumed to be common to all the environments, while the multipath models are different according to environments. A free space path model is employed, in which path loss for the distance between the transmitter and receiver equal to d $(d\ge 1)$ is given as

$$PL(d)=20\log_{10}(4\pi d f_c/c),\ f_c=\sqrt{f_{\min}f_{\max}} \quad (18)$$

where f_c denotes the geometric center frequency, with $f_{\min}$ and $f_{\max}$ being the lower and upper -10 dB frequencies of the power spectrum, and c is the speed of propagation. The shadow fading is assumed to follow a log-normal distribution with a log-standard deviation of 3 dB. For multipath fading, four different types of channel models, referred to as CM1, CM2, CM3 and CM4 corresponding to four kinds of environments, are defined based on the Saleh-Valenzuela model[13]. The main characteristics of these four channel models are listed in Table 2. The channel modeling subcommittee released 100 independent channel realizations for use in the

Table 2. Characteristics of multipath channel models based upon a sampling time of 0.167 nsec (CM1-4).

Channel Model	CM1	CM2	CM3	CM4
Environment	LOS 0-4 m	NLOS 0-4 m	NLOS 0-4 m	Extreme NLOS
Mean excess delay	5.0 nsec	9.9 nsec	15.9 nsec	30.1 nsec
RMS delay	5.0 nsec	8.0 nsec	15.0 nsec	25.0 nsec
Number of paths within 10 dB from the peak	12.5	15.3	24.9	41.2
Number of paths with 85% energy	20.8	33.9	64.7	123.3
Energy mean	-0.4 dB	-0.5 dB	0.0 dB	0.3 dB
Energy standard deviation	2.9 dB	3.1 dB	3.1 dB	2.7 dB

performance evaluation of UWB systems for each of these four channel models including the above-mentioned shadow fading[14]. Therefore, (18) is incorporated in all of our channel realizations.

4.2 Simulation Assumptions

Most of the assumptions follow those in [8]. We assume single link environments without inter-piconet interference. The payload size is fixed to 1024 bytes, and the roll-off factor β of a square-root raised cosine pulse is set to 0.3. The noise figure of the receiver is assumed to be 6.6 dB, and an implementation loss is assumed to be 2.9 dB. The transmit power is set to -9.9 dBm with zero back-off. The -10 dB cutoff frequencies in (18) are assumed to be $f_{\min}$ = 3100 MHz and $f_{\max}$ = 4850 MHz (lower band).

At the transmitter, BPSK modulation and convolutional encoding with constraint length 6 are assumed to be employed. The DFE is assumed to adopt a hard decision, and the decoding depth of the Viterbi decoder is fixed at 50 bits. The frequency and timing synchronization is assumed to be perfect at the receiver. The channel estimation is assumed to be perfect except for the results in Fig. 7.

4.3 Simulation Results

For a given channel model, frame error rate (FER) is estimated based on more than 100 independent trials for each of 100 channel realizations in [14]. As in [8], the performance is measured by 10% outage FER, i.e., the FER corresponding to the tenth worst channel among 100 channel realizations, versus the distance between the transmitter and receiver. In the following simulations, we consider two representative pairs of the channel model and transmission rate: (CM2, 220 Mbps) and (CM4, 110 Mbps), which are referred to as 'scenario 1' and 'scenario 2', respectively. Note that CM4 corresponds to more adverse channel environment than CM2, as summarized in Table II.

The effectiveness of the MMSE-DFE in the DS-UWB system is presented in Fig. 4 for both the two scenarios. For comparison purpose, we provide a matched filter bound (MFB), which can be closely

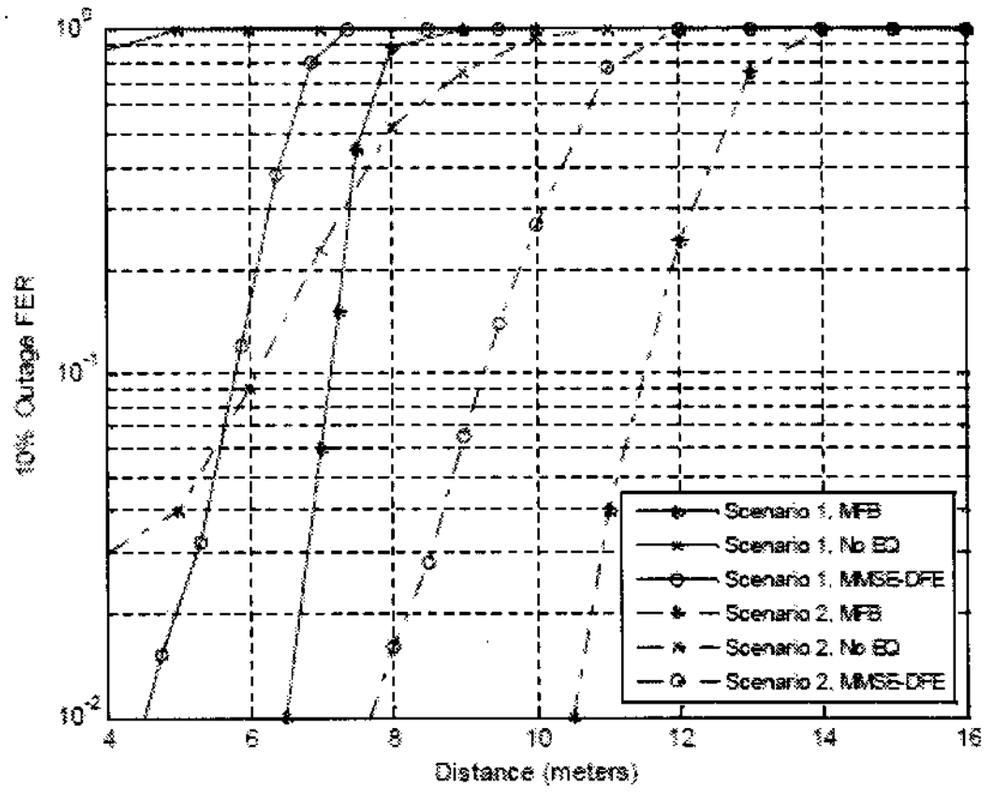

Fig. 4. The effectiveness of the MMSE-DFE in the DS-UWB system ($L=M=16$, $F=B=24$ for the scenario 1; $L=M=16$, $F=B=12$ for the scenario 2).

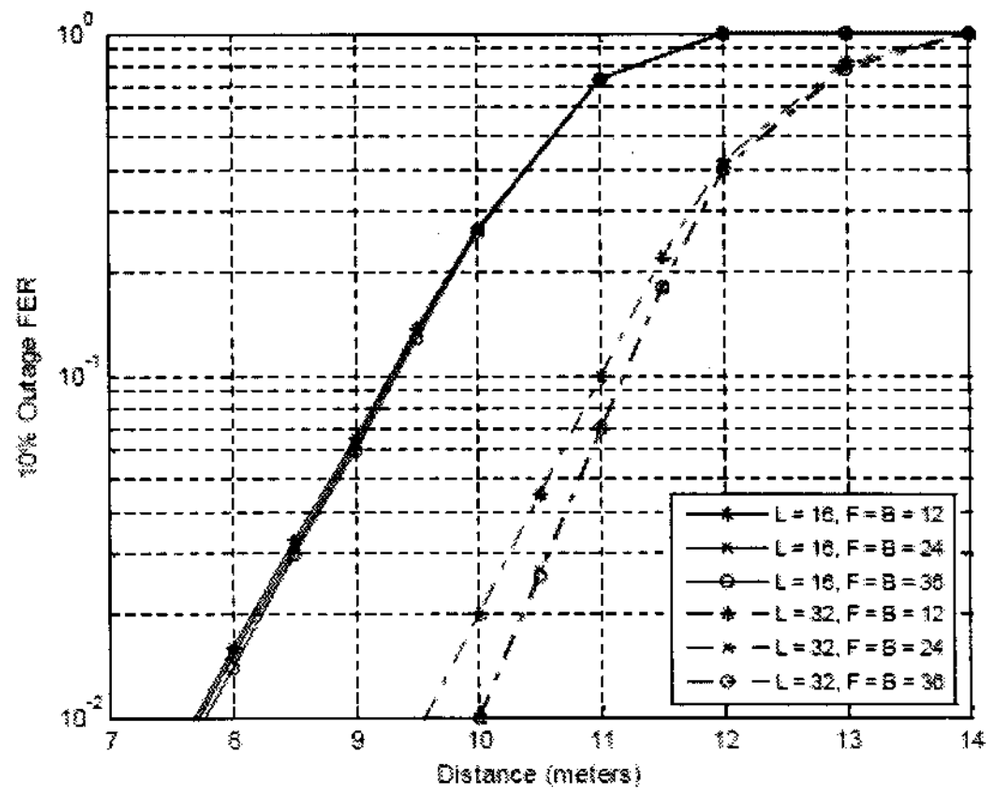

Fig. 5. The impact of the parameters L and (F, B) on the MMSE-DFE performance for the scenario 2.

approximated using an optimal equalizer like the maximum likelihood sequence estimator, and the results without equalization (No EQ). For the case of MMSE-DFE, we assume $L=M=16$ and $F=B=24$ for the scenario 1; $L=M=16$ and $F=B=12$ for the scenario 2. We observe that the use of MMSE-DFE significantly improves the performance of the DS-UWB system, although there is still a considerable gap from the MFB. This implies that the DS-UWB system may exhibit a range of performance depending on the performance of the equalizer, especially at high bit rates.

Fig. 5 shows the impact of the number of rake fingers L and the number of DFE taps F and B on the MMSE-DFE performance for the scenario 2. The

parameter M is assumed to be equal to L. Significant performance improvement is observed as L increases from 16 to 32. This is because the increase in L allows the receiver to collect more signal energy as well as to improve the equalizing capability. For the case of $L=16$, performance benefit obtained from larger number of filter taps is found to be negligible; $F=B=12$ is sufficiently large in the case. For the case of $L=32$, however, we observe substantial performance improvement when F and B increase from 12 to 24. These results imply that the more number of rake figures the receiver has, the more DFE filter taps is required to fully extract the gain due to the use of a DFE.

Figs. 6-7 show the impact of M, the number of paths used in deriving the coefficients of the MMSE-DEF, for both the scenarios. The number of rake fingers is fixed to $L=16$, and the number of DFE taps are set to $F=B=24$ for the scenario 1, and $F=B=12$ for the scenario 2. In Fig. 6, we assume perfect channel estimation, whereas in Fig. 7, channel estimation is performed using a sliding correlator [15] based on the nominal preamble [6]. When the channel estimation is perfect, the use of additional estimates suggested in Section III-3 is found to provide a substantial gain, especially for the scenario 2. In Fig. 6, for instance, the distances for achieving the 10% outage FER of 10^{-2} are about 7.7 m, 8.2 m, and 8.8 m, respectively, when M is

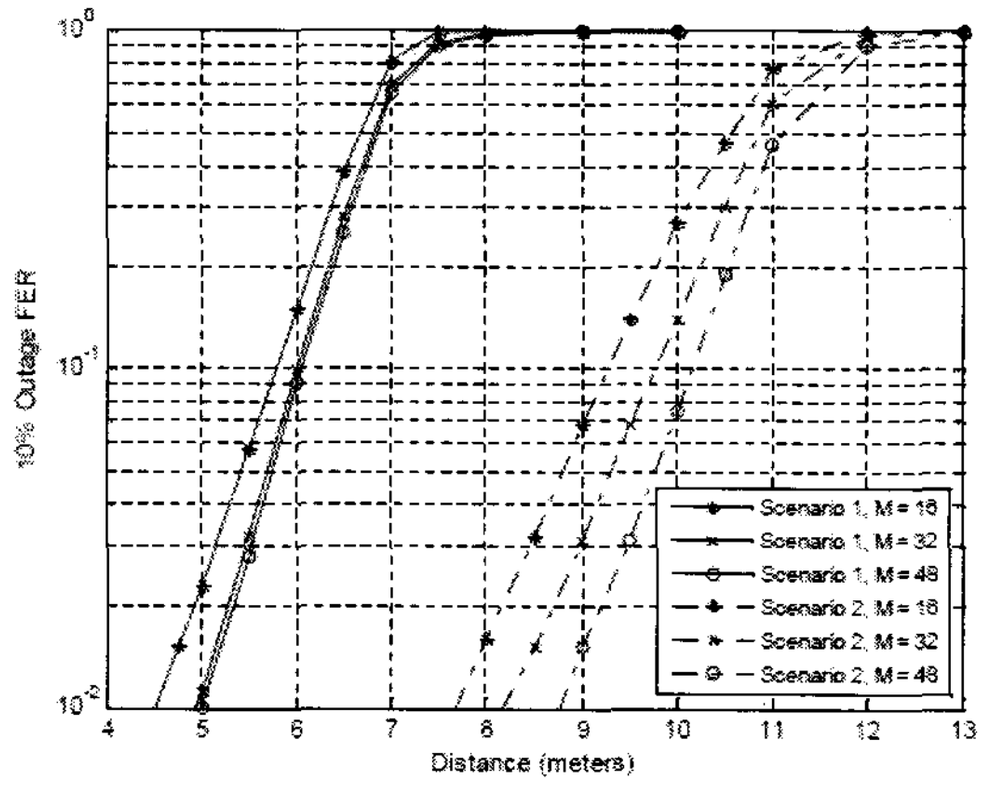

Fig. 6. The impact of the parameter M on the performance of MMSE-DFE with perfect channel estimation ($L=16$, $F=B=24$ for the scenario 1; $L=16$, $F=B=12$ for the scenario 2).

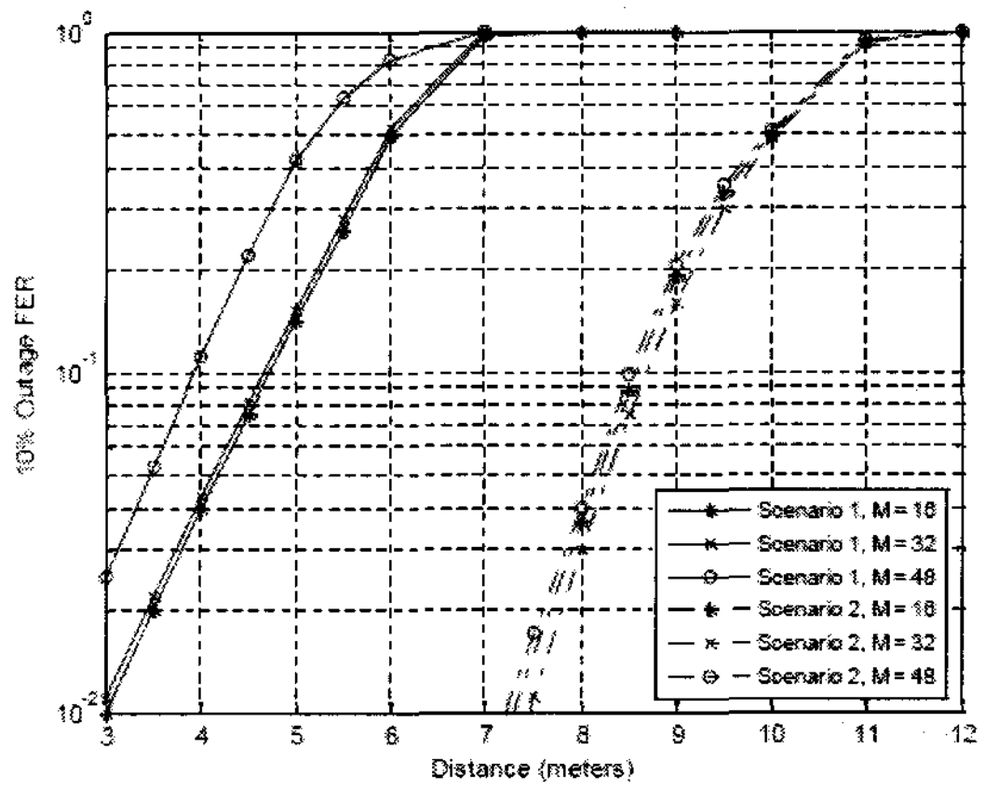

Fig. 7. The impact of the parameter M on the performance of MMSE-DFE with imperfect channel estimation ($L=16$, $F=B=24$ for the scenario 1; $L=16$, $F=B=12$ for the scenario 2).

equal to 16, 32, and 48. This amount of range extension can be translated into the energy gain of 1.2 dB when M increases from 16 to 48. When a sliding correlator is adopted for channel estimation, however, the advantage of using larger M is found to disappear. The use of M larger than L may even degrade the performance, as clearly seen from the scenario 1 in Fig. 7. The reason for this is that channel estimates for additional week paths with a sliding correlator will be too noisy to be helpful to the DFE performance. Hence, the parameter M must be carefully determined accounting for the accuracy of the channel estimation.

Fig. 8 shows the performance improvement owing

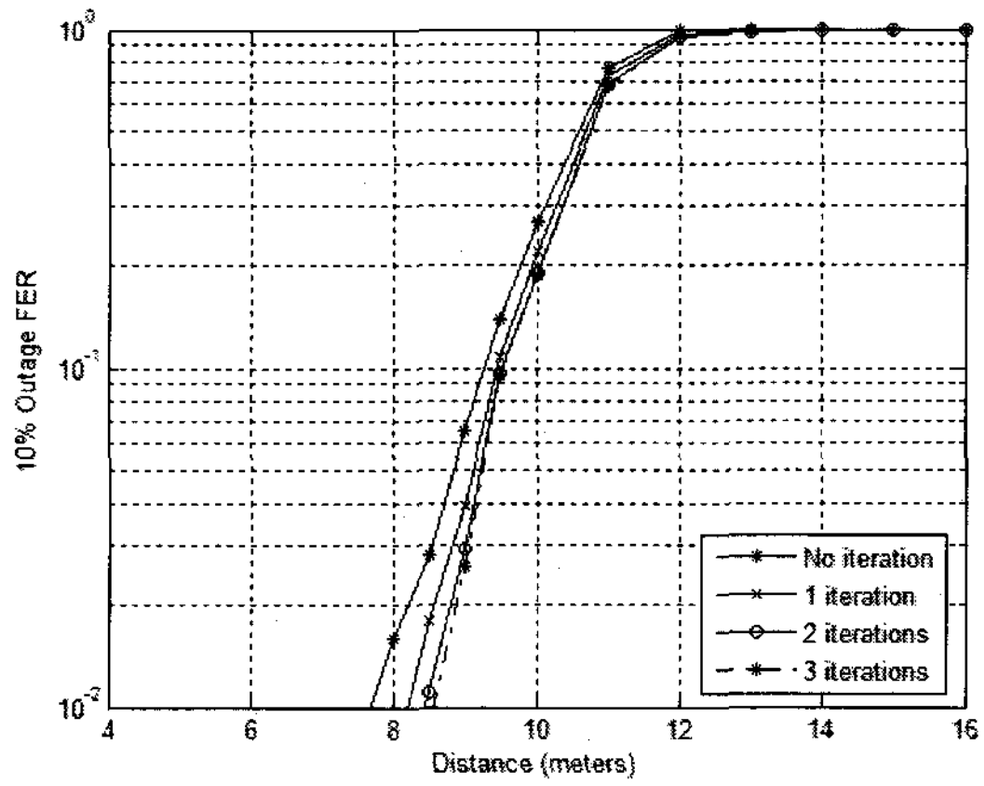

Fig. 8. The impact of the use of turbo equalization structure for the scenario 2 ($L=M=16$, $F=B=12$).

to the use of a turbo equalization structure in [10] for the scenario 2 with the same configuration of parameters as in Fig. 4. As expected, the FER decreases as the number of iterations increases. However, the improvement is shown to become marginal as the number of iterations goes up from two to three. This implies that in this case two iterations are enough to extract most of the gain due to turbo processing.

V. Conclusion

In this paper, we have investigated the performance of an MMSE-DFE for DS-UWB systems. We have derived the MMSE-DFE in the context of DS-UWB, and identified a key parameter that influences the performance of the MMSE-DFE. The performance of the MMSE-DFE has been evaluated with various parameters, such as the number of rake fingers, the number of DFE taps, and the number of additional channel estimates. In particular, we have found that the usefulness of additional channel estimates depends on the accuracy of the channel estimation. Indeed, the additional estimates are helpful to the MMSE-DFE, only when channel estimation is sufficiently accurate. We have also presented the performance improvement of the MMSE-DFE owing to the use of a turbo equalization structure.

References

[1] D. Porcino and W. Hirt, "Ultra-wideband radio technology: potential and challenges ahead," *IEEE Commun. Mag.*, Vol.41, pp.66-74, July 2003.

[2] C. R. Aiello and G. D. Rogerson, "Ultra-wideband wireless systems," *IEEE Microwave Mag.*, Vol.4, pp.36-47, June 2003.

[3] FCC, "First report and order in the matter of revision of part 15 of the commission's rules regarding ultra-wideband transmission systems," ET Docket No. 98-153, FCC 02-48, Apr. 2002.

[4] M. Z. Win and R. A. Scholtz, "Impulse radio: how it works," *IEEE Commun. Lett.*, Vol.2, pp.36-38, Feb. 1998.

[5] IEEE 802.15 high data rate alternative PHY task group 3a for wireless personal area networks, URL: http://www.ieee802.org/15/pub/TG3a.html.

[6] R. Fisher *et al.*, "DS-UWB physical layer submission to 802.15 task group 3a," IEEE P802.15-04/0137r5, Sept. 2005.

[7] C. Razzell *et al.*, "Multi-band OFDM physical layer proposal update," IEEE 802.15-04/0220r3, May 2004.

[8] O.-S. Shin, S. S. Ghassemzadeh, L. J. Greenstein, and V. Tarokh, "Performance evaluation of MB-OFDM and DS-UWB systems for wireless personal area networks," in *Proc. IEEE International Conference on Ultra-Wideband 2005*, Zurich, Switzerland, pp.214-219, Sept. 2005.

[9] A. Parihar, L. Lampe, R. Schober, and C. Leung, "Equalization for DS-UWB systems-Part I: BPSK modulation," *IEEE Trans. Commun.*, Vol.55, pp.1164-1173, June 2007.

[10] V. D. Trajkovic, P. B. Rapajic, and R. A. Kennedy, "Turbo DFE algorithm with imperfect decision feedback," *IEEE Signal Proc. Lett.*, Vol.12, pp.820-823, Dec. 2005.

[11] J. G. Proakis, *Digital Communications.* 4th ed., McGraw-Hill, New York, 2001.

[12] J. Foerster, "Channel modeling sub- committee report final," IEEE P802.15- 02/490r1, Feb. 2003.

[13] A. Saleh and R. Valenzuela, "A statistical model for indoor multipath propagation," *IEEE J. Select. Areas Commun.*, Vol.5, pp.128-137, Feb. 1987.

[14] UWB channel realizations for CM1-4, available online at ftp://ftp.802wirelessworld. com/15/Archive/2003/Mar03.

[15] A. A. D'Amico, U. Mengali, and M. Morelli, "Channel estimation for uplink of a DS-CDMA system," *IEEE Trans. Wireless Commun.*, Vol.2, pp.1132-1137, Nov. 2003.

신 오 순(Oh-Soon Shin) 정회원

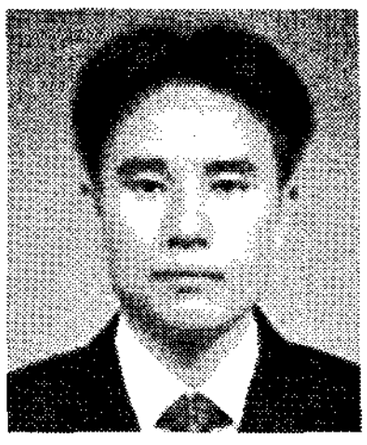

1998년 2월 서울대학교 전기공학부 학사

2000년 2월 서울대학교 전기공학부 석사

2004년 2월 서울대학교 전기컴퓨터공학부 박사

2004년 3월~2005년 9월 Harvard University 박사후 연구원

2006년 4월~2007년 8월 삼성전자 통신연구소 책임연구원

2007년 9월~현재 숭실대학교 정보통신전자공학부 전임강사

<관심분야> 통신이론, 통신시스템, 통신신호처리